ISSN 1054-660X, Laser Physics, 2009, Vol. 19, No. 2, pp. 371–376.

High-Energy Pulses from a Figure 8 Fiber Laser with Normal Net Dispersion[1]

O. Pottiez[a, *], B. Ibarra-Escamilla[b], and E. A. Kuzin[b]

[a] *Centre de Investigaciones en Óptica (CIO), Loma del Bosque 115, Col. Lomas del Campestre, León, Gto 37150, Mexico*

[b] *Institute Nacional de Astrofisica, Óptica o Electrónica (INAOE), L. E. Erro 1, Tonantzintla, Puebla, Pue 72000, Mexico*

*e-mail: pottiez@cio.mx

Received July 3, 2008

Abstract—In this paper we show numerically that high-energy pulses can be obtained with a figure-eight Erbium-doped fiber laser with large normal net dispersion, and in which an anomalous-dispersion Nonlinear Optical Loop Mirror (NOLM) is used as the effective saturable absorber. One advantage of this configuration over the ring cavity is the possibility to adjust the length of the NOLM loop to avoid overdriving the saturable absorber. The ring section of the laser includes a bandpass filter to balance the combined effects of Kerr nonlinearity and normal dispersion. Strict polarization control is performed in the NOLM as well as in the ring section of the laser. The NOLM is a power-symmetric scheme whose switching relies on nonlinear polarization rotation. This architecture allows a precise control of the low-power NOLM transmission through the orientation of a quarter-wave retarder, whose adjustment is shown to be critical for stable pulsed operation. Pulse formation appears to depend critically on the filter width. If it is wide enough, *ps* pulses with a large positive linear chirp are produced. After dechirping outside the laser, nearly transform-limited pulses with durations down to 240 fs, energies up to 10 nJ and peak powers beyond 40 kW are predicted.

PACS numbers: 42.55.Wd; 42.60.Fc; 42.65.Re

DOI: 10.1134/S1054660X09020339

1. INTRODUCTION

In spite of their high efficiency and insensitivity to alignment problems in comparison with solid-state lasers, mode-locked fiber lasers are discarded for some applications due to their limitations in pulse energy and thus in peak power, which result from the intrinsic fiber nonlinearity. In anomalous-dispersion femtosecond soliton fiber lasers [1], pulse formation results from a balance between Kerr nonlinearity and anomalous dispersion. The maximal pulse energy obtainable with these sources is ~0.1 nJ, as for high peak power pulse breaking occurs. In stretched-pulse fiber lasers, segments having opposite dispersion signs alternate to induce large periodic variations of pulse duration (pulse breathing) [2]. This procedure reduces the effective peak power in the cavity, and the maximal pulse energy is increased to a few nanojoules [3]. In the frame of stretched-pulse lasers, the benefits of the figure-eight (F8) laser over the ring configuration was demonstrated [4].

The highest pulse energies were obtained however with lasers operating in the large normal dispersion regime, although dechirping is required outside the laser [5]. In this regime, nonlinear phase shift and dispersion do not compensate each other but instead add up to induce a strong linear chirp on the pulse, sometimes called *self-similar pulse* [6–8]. Self-similar evolution induces a monotonous pulse widening, so that it must be balanced to ensure steady-state operation in a laser. This is made possible through the use of a bandpass filter, which stabilizes the pulse evolution by removing the frequency-shifted edges at each cycle [9]. Additional amplitude modulation is also provided by an effective saturable absorber (SA). The emerging pulses have durations in the ps range and a strong linear chirp. After dechirping is performed outside the laser through the use of the appropriate amount of anomalous dispersion, high-energy, high-peak-power, nearly transform-limited pulses with ~100 fs duration are obtained. Pulse energies above 10 nJ and peak powers close to ~100 kW were obtained in this regime [10]. Finally, another, non-self-similar regime was experimentally observed for large positive net dispersion, which also produces large pulse energies beyond 10 nJ [10, 11].

In these works, the passively mode-locked laser architectures were ring cavities, exploiting nonlinear polarization rotation (NPR) in the ring with a polarizer as the effective SA mechanism. Also, most of these lasers use Ytterbium-doped fiber as the amplifying medium, and thus emit at 1 μm. As standard fiber exhibits at this wavelength normal dispersion only, and because dispersion compensation is still needed in most schemes, an anomalous dispersion segment is included, which usually takes the form of a bulk grating pair, so that the resulting setup is not all-fiber and loses the ben-

[1] The article is published in the original.

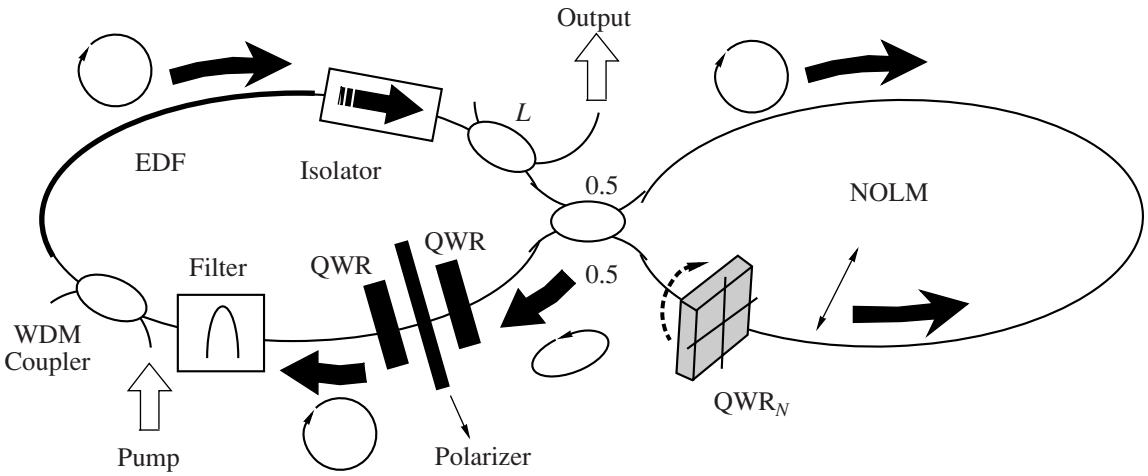

Fig. 1. Scheme of the laser under study.

efits of the waveguide medium. An all-normal-dispersion scheme was demonstrated experimentally, however the reported pulse energies of a few nanojoules did not exceed the performances of stretched-pulse fiber lasers [9].

In the present work we realize a numerical study of a F8 Erbium-doped fiber (EDF) laser designed to operate in the normal net dispersion regime. Considering the current availability of highly-doped broadband EDF, a doped fiber not longer than 5 m is considered. The doped fiber also provides the normal dispersion at 1550 nm. The SA action is due to a fiber Nonlinear Optical Loop Mirror (NOLM) [12]. One advantage of the F8 configuration over the ring cavity is that only the nonlinear phase shift in the NOLM loop (and not in the entire cavity) contributes to the SA action. Considering the interferometric nature of both NPR and NOLM (with a transmission that eventually decays at powers beyond the maximum), overdriving of the SA, which is one main cause of pulse energy limitation [4], can be avoided in the case of the NOLM simply by reducing its length. As standard fiber (presenting anomalous dispersion at 1550 nm) is used for the NOLM loop, it also ensures dispersion compensation. A bandpass filter is used in order to balance the pulse broadening associated with self-similar evolution.

2. MODEL

The F8 laser scheme under study is shown in Fig. 1. The NOLM is a power-symmetric structure whose operation relies on NPR instead of self-phase modulation (SPM) [13]. It consists of a symmetrical coupler, a piece of circularly birefringent fiber, and a quarter-wave retarder (QWR_N) located asymmetrically in the loop. Due to the QWR_N, the counter-propagating beams have different polarizations and accumulate different amounts of NPR, which allows switching. In practice, to prevent the nonlinear polarization evolution from averaging out for each beam during propagation, twist is applied to the fiber, which then becomes optically active and behaves like an ideal isotropic fiber [14]. The fiber inside the loop has a length L_N, an anomalous dispersion $D_N(\beta_{2N})$ and a nonlinear coefficient γ. The input polarization to the NOLM is circular, say right, and the orthogonal (left) circular polarization is selected at its output, through the use of a QWR and a polarizer. The combination NOLM + QWR + polarizer presents a sinusoidal nonlinear transfer characteristic, whose minimum and maximum values are 0 and 0.5, respectively, and whose low-power transmission can be adjusted precisely through the QWR_N orientation [15, 16]. Through the use of another QWR after the polarizer, polarization is made circular right. This polarization state is then maintained throughout the ring to the NOLM input. This can be realized in practice by twisting the ring section of the laser as well. The ring includes a Gaussian bandpass filter with full width at half maximum (FWHM) width $\Delta\lambda$, and a length L_A of EDF with appropriate low-signal gain and saturation energy, a normal dispersion $D_A(\beta_{2A})$ and nonlinear coefficient γ. The net cavity dispersion is normal: $L_N D_N + L_A D_A < 0$. An optical isolator and an output coupler introducing a loss L [coupling ratio = $1/L$:$(1 - 1/L)$] complete the ring.

Numerical simulations were performed to investigate the laser operation. Propagation in the NOLM and in the EDF was modeled using extended nonlinear Schrödinger equations, which were integrated using the Split-Step Fourier (SSF) method. In the NOLM, the clockwise (CW) beam is circularly polarized whereas the counter-clockwise (CCW) beam is linearly polarized after the QWR_N. This imposes the use of a set of two coupled nonlinear equations to describe propaga-

tion in the NOLM. In the circular polarization basis $[C^+, C^-]$, these equations write as

$$\frac{\partial C^+}{\partial z} = -j\frac{\beta_{2N}}{2}\frac{\partial^2 C^+}{\partial t^2} + \frac{2j\gamma}{3}(|C^+|^2 + 2|C^-|^2)C^+;$$
$$\frac{\partial C^-}{\partial z} = -j\frac{\beta_{2N}}{2}\frac{\partial^2 C^-}{\partial t^2} + \frac{2j\gamma}{3}(|C^-|^2 + 2|C^+|^2)C^-. \quad (1)$$

Right-hand sides of Eq. (1) include dispersive and Kerr nonlinear terms. The twist-induced group-velocity mismatch between circular polarization components, as well as higher-order effects like the Raman self-frequency shift and third-order dispersion were not accounted for, a valid approximation in the normal-dispersion regime, where pulses having durations of several ps are formed. Propagation in the EDF can be modeled using a single equation, as only one circular polarization component circulates in the ring. This equation writes as

$$\frac{\partial C^+}{\partial z} = \frac{g}{2}C^+ - j\frac{\beta_{2A}}{2}\frac{\partial^2 C^+}{\partial t^2} + \frac{2j\gamma}{3}|C^+|^2 C^+. \quad (2)$$

In addition to dispersive and nonlinear terms, Eq. (2) includes the gain term, where coefficient g is the gain per unit length. Here g is assumed to be constant across the EDF, and saturates on the pulse energy E_p as

$$g(E_p) = \frac{g_0}{1 + E_p/E_{\text{sat}}}, \quad (3)$$

where g_0 is the small-signal gain and E_{sat} is the saturation energy. The spectral dependence of gain is neglected, as its bandwidth is assumed to be larger than the filter bandwidth $\Delta\lambda$.

For various sets of laser parameters (dispersion map, NOLM length, QWR_N orientation, gain saturation energy, output coupler loss, and filter bandwidth), we investigated the conditions for stable pulse formation. In each case, a small-amplitude initial noise is propagated over several cycles, and we observe whether a steady-state can be reached or not after a finite number of integration cycles.

3. RESULTS AND DISCUSSION

Our analysis showed that the obtained results depend critically on the filter bandwidth $\Delta\lambda$. The highest pulse energy and peak power after recompression outside the laser is obtained for $\Delta\lambda = 8.3$ nm. The EDF has a length $L_A = 5$ m, a dispersion $D_A = -40$ ps/nm/km, and the NOLM is characterized by $L_N = 4$ m and $D_N = 20$ ps/nm/km, yielding a net dispersion $L_N D_N + L_A D_A = -0.12$ ps/nm. For both the NOLM loop and the EDF the nonlinear coefficient $\gamma = 1.5$ W^{-1} km^{-1}. The QWR_N is adjusted to ensure a NOLM transfer characteristic that presents an initial growth from a low-power value of ~0.1. The EDF had a small-signal gain of 5000 ($g_0 = 1000/m$) and a saturation energy $E_{\text{sat}} = 0.2$ nJ. The output coupler loss = 5 (coupling ratio = 20:80), meaning that only 20% of the input light is re-injected in the NOLM. In spite of this, and of the short NOLM length, a relatively large fraction of the pulse energy is switched to the NOLM output in regime (32%, to be compared with the 50% maximal transmission). In contrast, the bandpass filter cuts off at each pass ~75% of the pulse energy from its spectral and temporal wings. This shows the importance of the filter action in the pulse shaping process.

Figures 2a–2c show the evolution of the pulse duration and of the time-bandwidth product in the cavity in regime. The time-bandwidth product of the transform limited pulse having the same power profile as the actual pulse is also shown for comparison [dotted curve in Fig. 2c]. Pulse parameters present broad variations in the cavity, reaching one minimum and one maximum in each cycle. This clearly distinguishes this regime from the stretched-pulse operation, where two maxima and two minima are found every round-trip. Inside the NOLM, each parameter splits into two curves, corresponding to the CW and CCW beams. Each pulse narrows as it propagates in the anomalous-dispersion loop, and the recombination of the counter-propagating beams at the NOLM output also yields substantial compression [thick dot in Figs. 2b–2c]. However the large positive chirp of the pulse does not cancel out or gets negative in the NOLM, due to the large normal net dispersion. This, together with the large loss of the output coupler, ensures that the pulse peak power remains sufficiently low in the NOLM loop to avoid pulse breaking. After the filter however, both pulse duration and spectral width are reduced in such a way that the resulting pulse is nearly transform-limited [thick dot in Figs. 2b–2c]. After the filter, the pulse gets widened and positively chirped again in the EDF.

At the laser output, the pulse has an energy of 10.5 nJ, and a strong positive linear chirp [Fig. 2d]. After dechirping through an anomalous dispersion of 0.136 ps/nm outside the laser, 14-fold pulse compression yields transform-limited pulses with 240 fs FWHM duration and ~43 kW peak power. The approximately parabolic temporal profile of the output pulse, together with the nearly linear chirp, are signatures of the self-similar operation [5], as well as the optical spectrum with approximately parabolic top and steep edges [Fig. 2e]. Note finally that the output pulse spectrum is much wider than the filter bandwidth, confirming the strong filtering effect that is at play in the laser.

We investigated the dependence of the laser operation on the optical bandwidth. For $\Delta\lambda \le 5$ nm, no stable operation is observed, as the spectral narrowing action of the filter becomes too strong and no longer allows pulses to develop. On the other hand, for larger bandwidth values, stable solutions can be found. Figure 3 shows an example for $\Delta\lambda = 16.6$ nm. Parameters are the same as Fig. 2, except that low-power NOLM transmis-

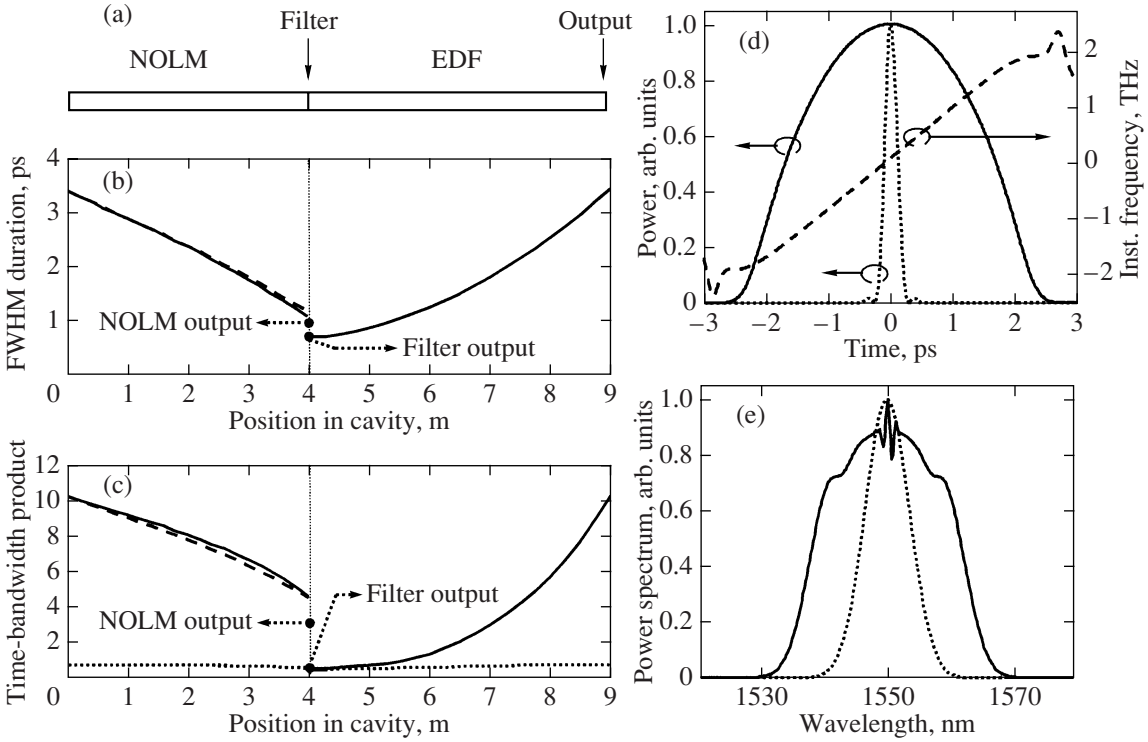

Fig. 2. (a) Schematic diagram of the laser; (b) FWHM pulse duration and (c) time-bandwidth product of the pulse along the cavity. Inside the NOLM, dashed and solid lines correspond to CW and CCW beams, respectively; dotted line shows the time-bandwidth product of the transform-limited pulses; parameters at the NOLM output and at the filter output are also marked by thick dots; (d) normalized pulse power profile at the laser output (solid) together with instantaneous frequency (dashed), and normalized power profile of the dechirped pulse (dotted); (e) output pulse spectrum (solid) and filter transmission spectrum (dotted). FWHM filter bandwidth $\Delta\lambda = 8.3$ nm. Other laser parameters are given in the text.

sion = 0.025 and $E_{sat} = 0.1$ nJ. In this case, although the role of the filter remains essential, its effect on the spectral shape is less drastic than in the case of Fig. 2, and only ~35% of the pulse energy is filtered out at each pass [see also Fig. 3e]. Although substantial pulse compression occurs both at the NOLM output and through the filter [thick dots in Figs. 3b–3c], the pulse at the filter output is now far from transform-limited. The output pulse energy however (6.4 nJ) is smaller than in the case of Fig. 2. In this case, only a small fraction not higher than 10% of the pulse energy is switched by the NOLM. If an attempt is made to increase the saturation energy or the NOLM length, stable solutions are no longer obtained. After dechirping outside the laser, 10-fold pulse compression is possible, yielding a transform-limited pulse with 340 fs FWHM duration and 16 kW peak power.

Another interesting result of our study is the importance of the NOLM adjustment for proper pulsed operation. Through the QWR_N orientation, the phase of the NOLM transfer characteristic, and thereby the low-power transmission can be adjusted between 0 and 0.5. A well known result is that, if low-power NOLM transmission is too low, intracavity power can not build up from initial noise because the small-signal losses in each cycle exceed the value of small-signal gain. With the parameters of Fig. 2, the minimal NOLM low-power transmission still allowing signal buildup is $\sim 10^{-3}$, a value consistent with the small-signal gain = 5000 and the output coupler loss = 5. If small-power NOLM transmission exceeds this value, stable pulses can be formed, provided that the sign of the bias ensures SA action (transmission growing with power), and not intensity-limiting action (compare curves A1 and B1 in [16, Fig. 3]). If low-power transmission is increased above 0.1, however, single-pulse operation is lost, so that the case of Fig. 2 corresponds to an upper limit of the QWR_N angle. Just above this value, a pattern consisting of several (2–3) pulses tends to appear, although no convergence was observed. The small value of this upper limit (corresponding to a QWR_N rotation of $\pi/16$ only from the position of zero low-power transmission) may be surprising, considering that the NOLM operation is clearly of the SA kind at this point, and that the maximum slope of the nonlinear characteristic at low power is only reached for a QWR_N rotation of $\pi/8$. From the analysis of the extensive simulations realized, this result can be understood by considering that a small value of low-power NOLM transmission is needed to prevent the growth of secondary

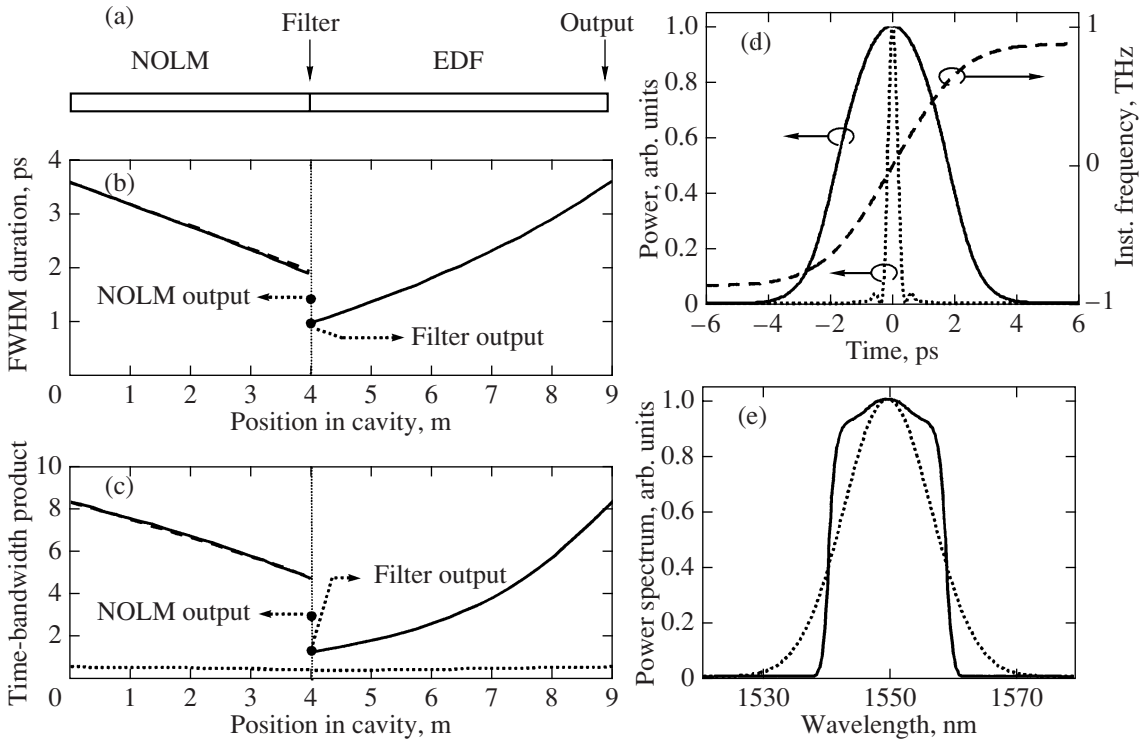

Fig. 3. Same as Fig. 2, for FWHM filter bandwidth $\Delta\lambda = 16.6$ nm. Other laser parameters are given in the text.

pulses that tend to emerge on the sides of the central high-powered pulse. In summary, the range of the QWR_N adjustment yielding a stable single pulse in the cavity appears to be quite narrow. This result could help understand recent experimental evidence that self-starting in a F8 laser with NPR-based NOLM only appears for a particular position of the QWR_N orientation [16].

4. CONCLUSIONS

In conclusion, we analyzed numerically an Erbium-doped F8 fiber laser designed for the generation of high-energy pulses. The device operates in the large normal dispersion regime, although the normal dispersion of the Erbium-doped fiber is partly compensated by the anomalous-dispersion NOLM. The self-similar pulse evolution due to Kerr nonlinearity and normal dispersion are balanced by the amplitude modulation of a bandpass filter, together with the SA action of the NOLM. Polarization control is implemented in the NOLM as well as in the ring segment of the laser. The NOLM is a power-symmetric, NPR-based setup, including an asymmetrically located QWR to break the polarization symmetry in the loop. By realizing polarization selection at the NOLM output, the nonlinear switching characteristic is a sinusoidal function of power with infinite dynamic range, and its low-power transmission can be adjusted through the QWR orientation. Simulations showed that wave-breaking-free pulsed operation was only possible in a narrow range of the QWR angle, showing that precise QWR adjustment is essential for proper operation of the laser. Simulations also revealed that the laser operation was very sensitive to the filter bandwidth. A very narrow filter does not allow pulse formation, whereas with a wide filter the pulse energy is limited to a few nanojoules. Using an intermediate value of ~8 nm for the filter bandwidth, ~3 ps pulses with a strong positive linear chirp are obtained, with a maximal pulse energy of ~10 nJ. After dechirping outside the laser, pulses with 240 fs duration and 43 kW peak power are obtained. This work could guide experimental research on all-fiber sources for the generation of high-power pulses at 1550 nm.

ACKNOWLEDGMENTS

O. Pottiez was supported by CONACyT grant 53990.

REFERENCES

1. I. N. Duling III, Electron. Lett. **27**, 544 (1991).
2. K. Tamura, E. P. Ippen, H. A. Haus, and L. E. Nelson, Opt. Lett. **18**, 1080 (1993).
3. L. E. Nelson, S. B. Fleischer, G. Lenz, and E. P. Ippen, Opt. Lett. **21**, 1759 (1996).

4. F. O. Ilday, F. W. Wise, and T. Sosnowski, Opt. Lett. **27**, 1531 (2002).
5. F. O. Ilday, J. R. Buckley, W. G. Clark, and F. W. Wise, Phys. Rev. Lett. **92**, 213902 (2004).
6. D. Anderson, M. Desaix, M. Karlsson, M. Lisak, and M. L. Quiroga-Teixeiro, J. Opt. Soc. Am. B **10**, 1185 (1993).
7. V. I. Kruglov, A. C. Peacock, J. M. Dudley, and J. D. Harvey, Opt. Lett. **25**, 1753 (2000).
8. V. I. Kruglov, A. C. Peacock, J. D. Harvey, and J. M. Dudley, J. Opt. Soc. Am. B **19**, 461 (2002).
9. A. Chong, J. Buckley, W. Renninger, and F. Wise, Opt. Exp. **14**, 10095 (2006).
10. J. R. Buckley, F. W. Wise, F. Ö. Ilday, and T. Sosnowski, Opt. Lett. **30**, 1888 (2005).
11. F. O. Ilday, J. R. Buckley, H. Lim, F. W. Wise, and W. G. Clark, Opt. Lett. **28**, 1365 (2003).
12. N. J. Doran and D. Wood, Opt. Lett. **13**, 56 (1988).
13. E. A. Kuzin, N. Korneev, J. W. Haus, and B. Ibarra-Escamilla, J. Opt. Soc. Am. B **18**, 919 (2001).
14. T. Tanemura and K. Kikuchi, J. Lightwave Technol. **24**, 4108 (2006).
15. O. Pottiez, B. Ibarra-Escamilla, and E. A. Kuzin, Opt. Comm. **281**, 1037 (2008).
16. B. Ibarra-Escamilla, O. Pottiez, E. A. Kuzin, J. W. Haus, R. Grajales-Coutiño, and P. Zaca-Moran, Opt. Comm. **281**, 1226 (2008).